CHAPTER 140

A MODEL FOR BREACH GROWTH IN A DIKE-BURST

Paul J. Visser*

ABSTRACT

A mathematical model for sand-dike breach erosion is presented. The heart of the model is a modified Bagnold (1963) energetics-based sand transport conception combined with a simplified Galappatti and Vreugdenhil (1985) pick up mechanism for the suspended load. The model has been tested to three laboratory experiments. The agreement between model predictions and experimental results is surprisingly good. Prototype calculations are presented for the 73 m high sand-dike of a proposed pumped-storage plant in the Netherlands.

1. INTRODUCTION

One of the possibilities for storage of energy is a water reservoir with a relatively high water level. In a flat country as The Netherlands a pumped-storage plant can be built by constructing an artificial basin surrounded by dikes. A proper location for the plant is along the coast against the Brouwersdam in the south-western part of The Netherlands. Recent feasibility studies conclude that the optimum dimensions of the reservoir are an area of about 15 km^2 and a water depth of about 70 m (resulting in a storage capacity of 20000 MWh and an electric power of 2000 MW). The ring-dike of the basin should be constructed with local sand ($D_{50} \approx 0.20$ mm).

Failure of the basin dike can result in a major disaster for the surroundings of the plant with losses of both human life and property. The possible consequences of an eventual dike-burst are important aspects for the determination of the exceptable failure probability of the basin. These consequences will depend on the behaviour of the flood wave, which in its turn will depend on the reservoir outflow hydrograph, particularly the maximum rate of outflow. The outflow hydrograph is governed largely by the growth of the breach with time.

The problem is comparable with that of earth-dam failures, for which the last 20 years a number of mathematical models has been developed, see Singh and Scarlatos (1988). These models, as also the model of Fujita and Tamura (1987) for the breaching of bursts in river

* Scientific Officer, Department of Civil Engineering, Delft University of Technology, P.O. Box 5048, 2600 GA Delft, The Netherlands.

dikes, assume bed load as the prevailing transport mechanism. But in case of failure of a high sand–dike suspended load transport will dominate. Since this results in a completely different breach erosion, these models cannot be applied here.

The aim of the investigation is a mathematical model which describes the growth of the breach and the discharge with time. The study was done for the NOVEM (Netherlands Company for Energy and Environment).

Starting point is a basin with an area of 15 km² and a water depth H_w = 70 m. It is assumed that the 73 m high ring–dike is

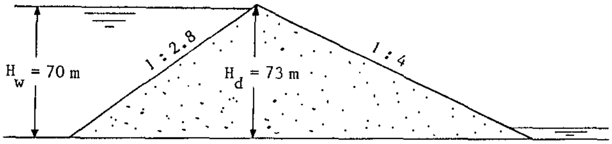

Fig. 1 Schematization of the cross–section of the high sand–dike

completely built up with sand (D_{50} = 0.20 mm), see Fig. 1. The inner and outer slopes are 1 : 2.8 and 1 : 4, respectively. All these quantities can also be varried. It is further assumed that the dike–burst starts with a small initial breach at the crest of the dike, for instance due to piping.

2. DESCRIPTION OF SAND TRANSPORT

A proper description of the pick up and transport of sediment is essential for the simulation of breaching processes. In the case of failure of the sand dike of a 70 m high reservoir, the outflow velocities will become very large (order of magnitude 20 m/s). None of the existing sediment transport formulae has been verified for these velocities. Hence, an energetics–based approach is applied in which the sand transport is expressed directly in the available power for it from the flow. Thus, a huge overestimation of the sand transport (as by some other formulae) is prevented.

The present approach is based on the energetics–based sediment transport conception of Bagnold (1963, 1966). The incorporation of the slope effect differs ,however, from Bagnold's (1963) approach.

Bagnold expressed the sediment transport in the available energy ω per unit time and unit area of the bed surface:

$$\omega = \tau_b = C_f \rho u^3 \qquad (1)$$

where τ_b is the bed shear stress, u is the depth–averaged current velocity, C_f is the drag coefficient for the bed ($\approx$ 0.01) and ρ is the water density.

The Bagnold conception includes both bed load transport (capacity s_b) and suspended load transport (capacity s_s). Here the order of magnitude of the ratio s_b/s_s will be:

$$\frac{s_b}{s_s} \approx \frac{13}{tg\phi}\frac{W}{u} \approx \frac{13}{0.6}\frac{0.02}{20} \approx 0.02 << 1 \qquad (2)$$

where ϕ is the internal angle of friction of the sediment in the bed load ($\phi \approx 32°$ for sand) and W is the fall velocity of the sediment. So the bed load transport can be neglected with respect to the suspended load transport.

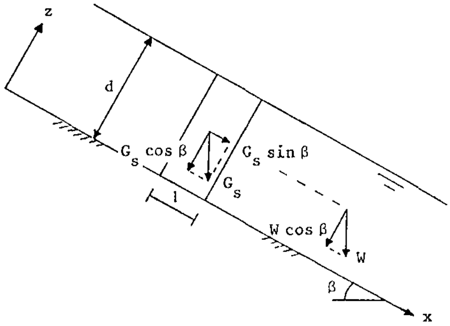

Fig. 2 Components $G_s \cos \beta$ and $W \cos \beta$ normal to the slope of G_s and W, respectively

Consider a column of water in the flow on a slope (with angle β) with an unit area of 1 m² (along the slope) and a height d equal to the water depth, see Fig. 2. If C_s is the immersed weight of the suspended material within this column and u_s is the average transport velocity of these solids, then the suspended load transport s_s, can be written as

$$s_s = C_s u_s \qquad [\text{N/ms}] \qquad (3)$$

The lifting work P (per unit time and unit width) by the turbulence which is required to keep the solids in suspension is

$$P = (C_s \cos \beta)\ (W \cos \beta) \qquad (4)$$

This work is delivered by ω; however, only a (small) part of ω is used for this:

$$P = e\ \omega \qquad (5)$$

where e is the efficiency factor for the suspended load transport (e = 0.01 according to Bagnold, 1966).

Combining (1), (3), (4) and (5) yields

$$s_s = \frac{0.01\ C_f\ \rho\ u_s\ u^3}{W \cos^2 \beta} \qquad [\text{N/ms}] \qquad (6)$$

The effect of the weight component $G_s \sin \beta$ is that the suspended sediment will push the fluid along instead of vice versa. So $u_s > u$, but the difference will be small ($u_s \approx u$). Hence it is assumed that the contribution of $G_s \sin \beta$ to the lifting work P is negligible. This approach differs from that of Bagnold (1963) and Bailard (1981) who assumed contributions to P of $G_s \sin \beta\ u_s$ and $e\ C_s \sin \beta\ u_s$, respectively.

The weight of 1 m³ sand under water is: $(1 - p)(\rho_s - \rho)\,g$ [N], in which p is the porosity, ρ_s is the sediment density and g is the acceleration of gravity. Now (6) can be written as:

$$s_s = \frac{0.01\, C_f\, u^4}{(1 - p)\,\Delta\, g\, W \cos^2 \beta} \qquad [m^2/s] \qquad (7)$$

in which $\Delta = (\rho_s - \rho)/\rho$. Equation (7) applies to the capacity of the suspended load transport. There remains the description of the process of pick up of sediment up to this capacity.

Fig. 3 shows schematically the two-dimensional situation of flow and sand transport on the outer or downstream slope in a stage which differs only slightly from the initial state (slope 1 : 4).

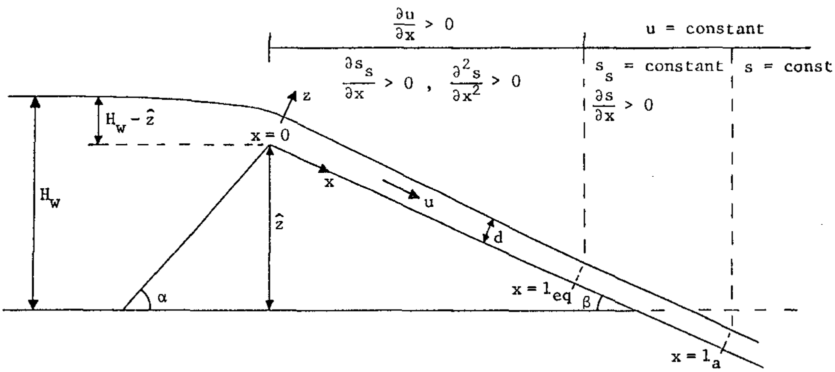

Fig. 3 Schematization of flow and sand transport on the downstream slope

The crest acts as a weir, the flow over it is critical. On the downstream slope, where the flow is super-critical, the current accelerates up to a distance $x = \ell_{eq}$ from the crest (x is the coordinate along the slope, x = 0 at the crest); there the current velocity reaches the equilibrium value for uniform flows

$$u_{eq} = \left(\frac{g\, d \sin \beta}{C_f} \right)^{1/2} \qquad (8)$$

Upstream from the crest the sand transport is very small (in the experiments) or nothing at all (in practice, due to the revetment of the slope). The entrainment of sediment in suspension starts at the crest. For $x = \ell_a$ (= adaption length) the suspended load transport reaches its capacity; naturally ℓ_a can be larger than L (= length of downstream slope), and always $\ell_a \gtrless \ell_{eq}$ due to the adaption process of the suspended load.

A description of the entrainment process for sediment in suspension is given by Galappatti and Vreugdenhil (1985). For small values of W/u_* as in the present situation, i.e. $W/u_* = W/(\sqrt{C_f}\, u) \approx 0.01$ (see (2), u_* is the bed shear velocity), their theory can simply be approximated as

$$s(x) = \frac{x}{\ell_a}\, s_s \qquad \text{for} \qquad 0 \le x \le \ell_a \qquad (9)$$

where (with q is the outflow rate per unit width):

$$\ell_a = \frac{u\ d}{W \cos \beta} = \frac{q}{W \cos \beta} \tag{10}$$

3. MATHEMATICAL MODEL

3.1 Outflow rate

The maximum outflow rate Q_{max} will occur for large values of the water depth H_w in the reservoir, see Fig. 11. Then the flow in the breach is still critical, so the equation for the rate of outflow is:

$$Q = q\ b = m_o \frac{2}{3} \left(\frac{2}{3}\ g\right)^{1/2} b\ H^{3/2} \tag{11}$$

where m_o is the discharge coefficient (≈ 1.0), b is the average breach width and $H = H_w - \hat{z}$ ($\hat{z}$ is the height of the breach top above the reservoir bottom, see Fig. 3).

3.2 Growth of breach in depth

The equation describing the erosion of the downstream slope is

$$\frac{\partial z_b}{\partial t} + \frac{\partial s}{\partial x} = 0 \tag{12}$$

where t is the time and $z_b = z_b(x, t)$ is the position of the sloping bottom in z–direction (z is the coordinate normal to the slope).

The suspended load capacity s_s increases for $0 < x < \ell_{eq}$ since u accelerates here. This means with (9) and (12)

$$\frac{\partial}{\partial x}\left|\frac{\partial z_b}{\partial x}\right| = \frac{\partial^2 s}{\partial x^2} > 0 \qquad \text{for} \qquad 0 < x < \ell_{eq} \tag{13}$$

i.e. the rate of erosion increases along the slope. Hence the downstream slope becomes steeper with increasing x and in time, see Fig. 4.

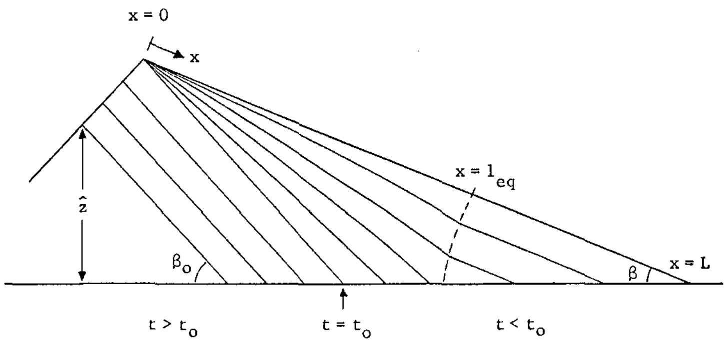

Fig. 4 Erosion of the downstream slope

If it is assumed that C_f and β are constant, then s_s is constant for $\ell_{eq} < x < \ell_a$ since u is constant here, see (7). This means that

$$\frac{\partial}{\partial x}\left|\frac{\partial z_b}{\partial t}\right| = 0 \qquad \text{for} \qquad \ell_{eq} < x < \ell_a \tag{14}$$

i.e. the rate of erosion is constant along this part of the slope, see Fig. 4.

Fig. 4 shows also the result of the above described development: the downstream slope becomes steeper and steeper. The steepness of the slope will not exceed, however, a certain limit tg β_o. If this limit has been achieved on the entire slope (on $t = t_o$), then the erosion rate becomes also constant for $0 < x < \ell_{eq}$, see the straight lines in Fig. 4 for $t > t_o$. Thus, for $t \geq t_o$ the erosion of the downstream slope is completely determined by the erosion at $x = \ell_{eq}$, i.e. by the erosion at the toe of the slope (x = L):

$$- L \frac{dz_b}{dt} = s_L \qquad \text{for} \qquad t \geq t_o \tag{15}$$

where with (9):

$$s_L = \frac{L}{\ell_a} (s_s)_L \tag{16}$$

Substitution of d = q/u into (8) gives for the current velocity at x = L:

$$u_L = \left(\frac{g\ q \sin \beta}{C_f}\right)^{1/3} \tag{17}$$

The relation between the fall dz of the breach top and the erosion dz_b of the downstream slope follows from a simple geometrical

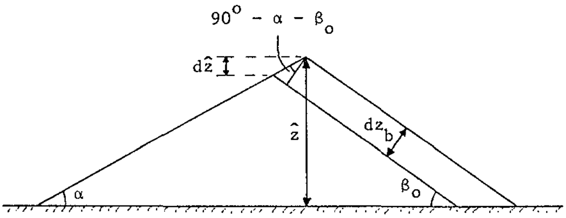

Fig. 5 Relation between $d\hat{z}$ and dz_b

consideration, see Fig. 5:

$$\frac{d\hat{z}}{dt} = \frac{\sin \alpha}{\sin (\alpha + \beta_o)} \frac{dz_b}{dt} \tag{18}$$

Substitution of (15), (16), (7), (10), (17), $\beta = \beta_o$ and (11), successively, into (18) gives:

$$\frac{d\hat{z}}{dt} = -k\,H^{\frac{1}{2}} = -k\,(H_w - z)^{\frac{1}{2}} \text{ for } t \geq t_o \tag{19}$$

$$\text{where} \quad k = 0.0082\,\frac{(g)^{\frac{1}{2}}}{\Delta\,(1-p)}\,\left(\frac{m_o}{C_f}\right)^{1/3}\,\frac{\sin\alpha\,(\sin\beta_o)^{4/3}}{\sin(\alpha+\beta_o)\,\cos\beta_o} \tag{20}$$

3.3 Growth of breach width

Consider the small initial breach $A_oB_oC_oD_o$ of Fig. 6 with an average width b_o, a bottom width a_o and a height h_o. It is assumed that the angle of the side slopes is somewhat smaller than the angle of repose ϕ. The direction of the flow through the breach is perpendicular to the paper.

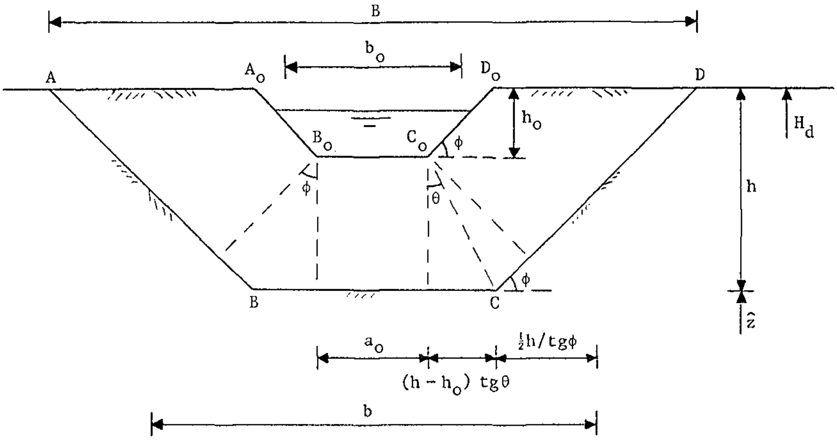

Fig. 6 Assumed growth of breach ABCD from initial $A_oB_oC_oD_o$

The rate of erosion down below the side slopes is larger (due to larger current velocities) than higher on the slopes. This means that the slopes become steeper and steeper, until the situation gets unstable and the sides will slide into the channel. This is in accordance with the observations (which are described in chapter 4). Thus, it is assumed that the angle of the side slopes is constant and equal to ϕ. Hence, if the sand dike is homogeneous then the initial breach $A_oB_oC_oD_o$ will develop into the breach ABCD with an average width b:

$$b = a_o + 2\,(h - h_o)\,tg\,\theta + \frac{h}{tg\,\phi} \tag{21}$$

and width B at the crest of the dike:

$$B = a_o + 2\,(h - h_o)\,tg\,\theta + \frac{2h}{tg\,\phi} \tag{22}$$

in which h is the breach depth and $0 < \theta < \phi$.

If $b_o << b$ and $h_o << h$, then (21) and (22) can be written as:

$$\frac{b}{h} \approx 2 \text{ tg } \theta + \frac{1}{\text{tg } \phi} \tag{23}$$

$$\frac{B}{h} \approx 2 \text{ tg } \theta + \frac{2}{\text{tg } \phi} \tag{24}$$

For sand: $\phi \approx 32^0$ Thus, with $0 < \theta < \phi$:

$$1.6 < \frac{b}{h} < 2.9 \tag{25}$$

$$3.2 < \frac{B}{h} < 4.4 \tag{26}$$

If the rate of erosion just left from the point C_o equals to that just right from this point then $\theta = \phi/2$ and

$$\frac{b}{h} \approx 2.2 \text{ and } \frac{B}{h} \approx 3.8 \tag{27}$$

If the breach is schematized as shown in Fig. 7, then it

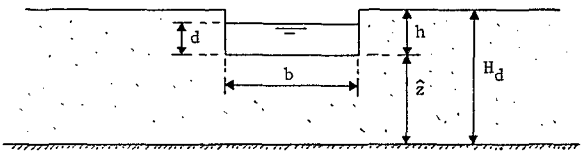

Fig. 7 Schematization of the breach

follows from the foregoing that the breach width b is simply related to the breach depth

$$b = r\ h = r\ (H_d - \hat{z}) \tag{28}$$

where r is a constant with a theoretical value of about 2.2 and H_d is the height of the dike.

The continuity equation for the total sediment transport S through the breach channel reads

$$\frac{\partial S}{\partial x} - \frac{\partial bh}{\partial t} = 0 \tag{29}$$

where (see Fig. 7):

$$S = s(b + 2d) \tag{30}$$

Substitution of (28) and (30) into (29) gives with $\partial h/\partial t = - \partial z_b/\partial t$ and the assumption that b and d are nearly constant along the slope:

$$\frac{b + 2d}{2b} \frac{\partial s}{\partial x} + \frac{\partial z_b}{\partial t} = 0 \tag{31}$$

i.e. (19) should be corrected to

$$\frac{d\hat{z}}{dt} = - \frac{b + 2d}{2b} k H^{\frac{1}{2}} = - f k H^{\frac{1}{2}} \qquad (32)$$

Thus, $d\hat{z}/dt$ slows down with a factor f compared with the 2-dimensional situation. The factor f can be calculated for any $\hat{z}$ from $d = q/u_L$, (11), (17) and (28).

3.4 Decrease of reservoir water depth

The decrease of the water depth in the reservoir follows simply from the equation describing continuity of mass:

$$A \frac{dH_w}{dt} = - Q \qquad (33)$$

or with $H_w = H + \hat{z}$:

$$\frac{dH}{dt} + \frac{d\hat{z}}{dt} = - \frac{Q}{A} \qquad (34)$$

The equations (32) and (34) form a system of coupled differential equations for H and $\hat{z}$.

4. EXPERIMENTS

Three experiments were performed for the verification of the model. Fig. 8 (lines for t = 0) shows the cross-section of the dike at

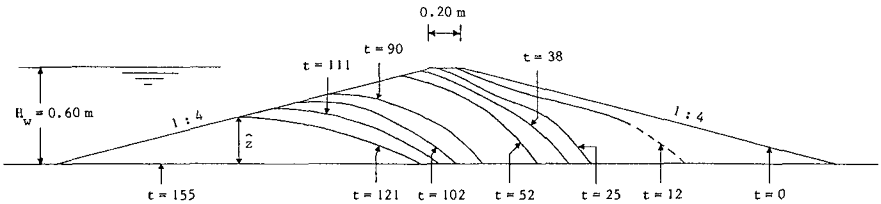

Fig. 8 Cross-section of the dike in the breach on different times t (in seconds) in Exp. 3

the start of each experiment, completely built up with sand: D_{50} = 0.10 mm in Exp.'s 1 and 3, D_{50} = 0.20 mm in Exp. 2. The upstream water depth was kept constant at 0.60 m, the downstream water depth at the start of the experiments was nil. The breach growth was video taped because of the very rapid process of breaching.

Exp. 1 was done in a large (wave) basin in which a 6 m long dike was constructed. The dike-burst started at t = 0 with the flow through a small initial channel in the crest of the dike. Fig. 9 shows the top width B(t) of the breach as observed from the video tape.

Exp.'s 2 and 3 were performed in a flume with a width of 0.50 m. Exp. 3 is a two-dimensional experiment: the erosion of the dike took place over the total width of the flume. The observed development of the downstream slope (see Fig. 8) is in agreement with the reasoned one (see Fig. 4). The downstream slope in Exp. 3 became steeper until

$t = t_o = 25$ s without any appreciable drop of the crest. Fig. 10 shows the observed top height $\hat{z}(t)$ in Exp. 3.

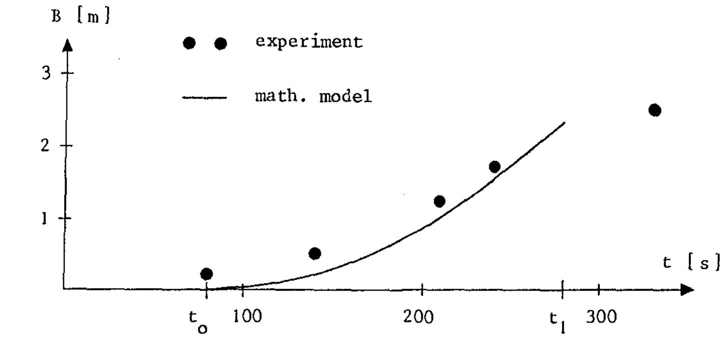

Fig. 9 Observed (Exp. 1) and theoretical top width B(t) of the breach

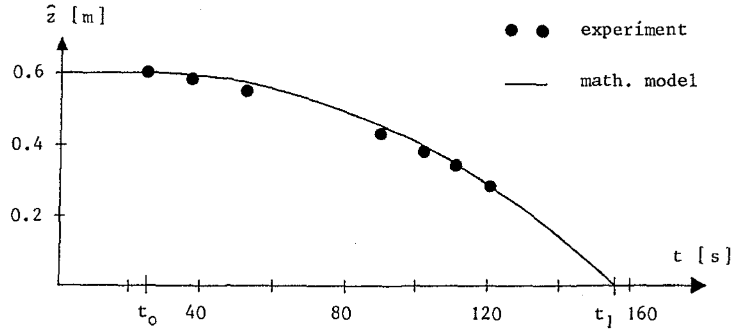

Fig. 10 Observed (Exp. 3) and theoretical top height $\hat{z}(t)$

5. VERIFICATION AND RESULTS

5.1 Comparison with experiments

The present breach erosion model has been verified to the data of the three experiments. In this paper only the testing for Exp.'s 1 and 3 is briefly described. As stated in chapter 3, the model can be applied after the steepening of the downstream slope, i.e. for $t > t_o$.

Fig. 10 shows the comparison of the computed and observed crest height $\hat{z}(t)$ of the dike in the breach. The calculation was done for H_w = constant = 0.60 m , t_o = 25 s , $\alpha = 14^o$, $\beta_o = \phi = 32^o$, m = 1.2 , $\Delta = 1.65$, p = 0.4 , $\hat{f}$ = 1 (2-dimensional) and $C_f = 0.06$. The rather large value of 0.06 for C_f was computed with (17) and u = q/d using the observed water depths on the crest of the weir (for q) and on the downstream slope in an initial stage of Exp. 3. On $t = t_1 = 155$ s the dike in the flume was completely washed away.

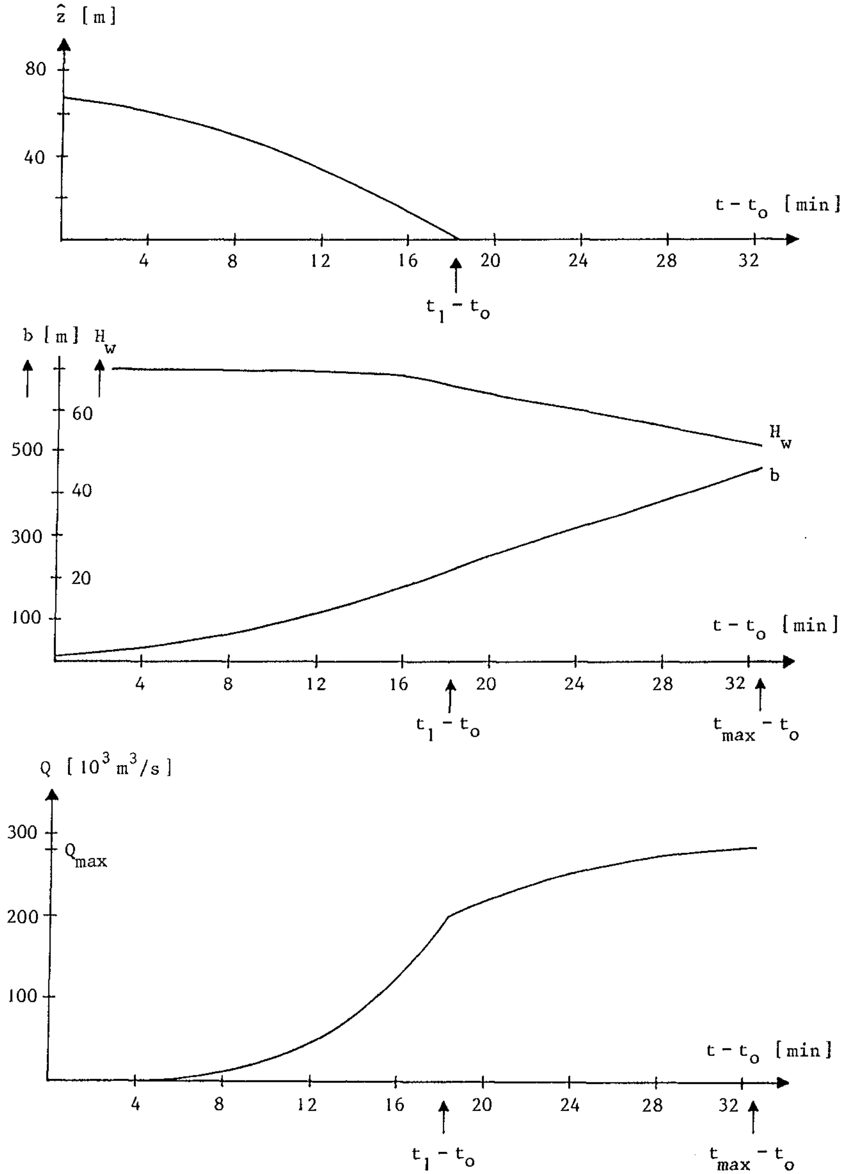

Fig. 11 Top height $\hat{z}(t)$, average breach width $b(t)$, reservoir water depth $H_w(t)$ and outflow rate $Q(t)$ as computed for the high sand-dike of Fig. 1.

The comparison of the computed and observed top width B(t) of the breach in Exp. 1 is shown in Fig. 9. The calculation was done for H_w = constant = 0.60 m , t_o = 80 s , $\alpha = 14^o$, $\beta_o = \phi = 32^o$, $m = 1.2$, $\Delta = 1.65$, $p = 0.4$, $C_f = 0.06$ and $B/h_o = 3.8$.

It can be concluded from Fig.'s 9 and 10 that the agreement between model predictions and experimental data is very good.

5.2 Prototype calculations

Since the model is based on the process of entrainment of sand on a relatively steep slope, its validity is also limited to $t < t_1$.

In the present calculations the model was simply applied for $t_1 \le t \le t_{max}$ too (t_{max} is the time where Q is maximal), i.e. (28) for b with (19) for $\hat{z}$. For the rate of outflow, however, it was assumed that if $\hat{z} < 0$ then Q is determined by H_w (i.e. in (11) $h = H_w$) and the length of the circular weir upstream of the scour hole and not influenced by the scour hole itself.

The results of the (numerical) computations for the sand-dike of the pumped-storage plant (H_w = 70 m , A = 15 km² , $\alpha = 19.6^o$) with the basic values for the different parameters ($\beta_o = \phi = 32^o$, $m = 1.0$, $\Delta = 1.65$, $p = 0.4$, $r = 3$, $e = 0.01$ and $C_f = 0.015$) are shown in Fig. 11. The relatively large value of 0.015 for C_f was measured by the Dutch Public Works Department in the field during the final phase of a "sand-closure", i.e. in a situation with large current velocities.

The duration t_o can be estimated from the measured t_o = 80 s in Exp. 1 and the time-scale factor for the morphological process.

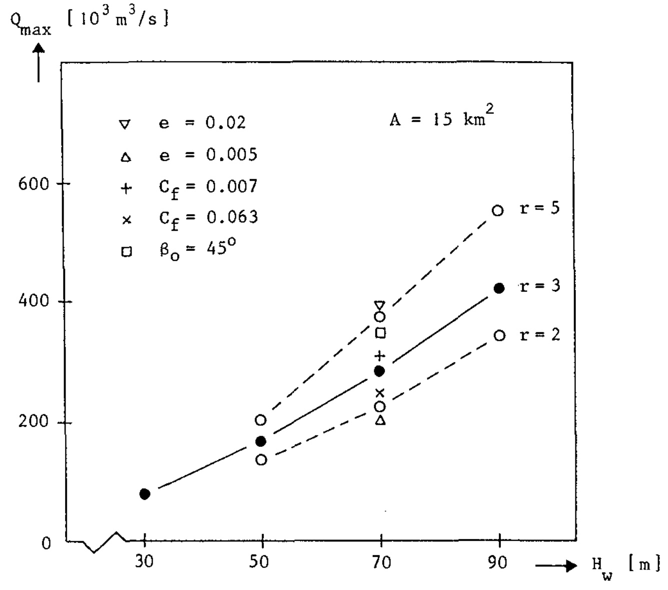

Fig. 12 Sensitivity of the computed Q_{max} for the different parameters

This gives t_o = 560 s = 9.3 min., see Visser, Ribberink and Kalkwijk (1986).

Thus, the model predicts for the outflow rate a maximum value:

$$Q_{max} = 2.8 * 10^5 \ m^3/s \quad \text{for} \quad t = t_{max} = 2.5 * 10^3 \ s = 42 \ min.$$

Fig. 12 shows the sensitivity of the computed Q_{max} for the different parameters, i.e. for the width/depth-ratio r of the breach, the efficiency factor e for the suspended load transport, the drag coefficient C_f for the bed, the critical slope angle β_o and the reservoir water depth H_w. The model is especially sensitive for e and r.

6. DISCUSSION

The output of the study is a relatively simple model for the simulation of sand-dike breach erosion. The investigation was done for the feasibility study of a pumped-storage plant in the Netherlands. The model predicts for the 73 m high sand-dike of the water reservoir the following failure scenario in case a small initial gap springs up at the crest on t = 0:

- $0 < t < t_o$: the slope angle β of the breach channel in the downstream slope will become larger,
- $t = t_o$ = 9 min.: β will reach a critical value β_o , the flow rate will be still small and the erosion of the top will start (the duration t_o is very sensitive to the initial conditions),
- $t_o < t < t_1$: erosion of the dike in the breach,
- $t = t_1$ = 28 min.: the dike in the breach will be completely washed away, $Q_1 \approx 2.0 * 10^5 \ m^3/s$,
- $t_1 < t$: the breaching process will continue in both vertical and horizontal direction; for the outflow rate Q the increase of the breach width is of importance,
- $t = t_{max}$ = 42 min.: $Q_{max} \approx 2.8 * 10^5 \ m^3/s$.

The model is based on the erosion process of a relatively steep slope ($t_o < t < t_1$) and was also tested as such to the results of three experiments. The agreement between model and experiments is surprisingly good.

For much lower dikes, as river or sea dikes, Q_{max} will generally be much larger than Q_1. It is clear that the modelling of the breach growth for $t > t_1$ should be improved before the model can be released for these dikes.

A sensivity analysis indicates that the efficiency factor e for the suspended load transport and the width/depth-ratio r of the breach are the most sensitive parameters in the model; e is the most uncertain parameter. Measurements on the pick up and transport of sediment at high velocities (≈ 10 m/s) should be done to reduce this uncertainty.

REFERENGES

Bagnold, R.A., 1963. Mechanics of marine sedimentation. In The Sea: Ideas and Observations, vol. 3, Interscience, New York, pp. 507–522.

Bagnold, R.A., 1966. An approach to the sediment transport problem from general physics. Geological Survey Professional Paper 422–I , U.S. Government Printing Office.

Bailard, J.A., 1981. An energetics total load sediment transport model for a plane sloping beach. Journ. Geophysical Res., vol. 86, pp. 10938–10954.

Fujita, Y. and Tamura, T., 1987. Enlargement of breaches in flood levees on alluvial plains. Natural Disaster Science, vol. 9, pp. 37–60.

Galappatti, R. and Vreugdenhil, G.B., 1985. A depth-integrated model for suspended sediment transport. Journ. Hydraulic Res., vol. 23, pp. 359–377.

Singh, V.P. and Scarlatos, P.D., 1988. Analysis of gradual earth-dam failure. Journ. Hydraulic Eng., vol. 114, pp. 21–42.

Visser, P.J., Ribberink, J.S. and Kalkwijk, J.P.Th., 1986. The development of the breach and rate of outflow in case of dike failures (in Dutch). Rep. 8-86, Hydraulic Eng. Group, Fac. of Givil Eng., Delft Univ. of Techn.

AGKNOWLEDGEMENT

The work upon which this paper is based was supported in part by the NOVEM B.V. (Dutch Gompany for Energy and Environment).